Development of Quantum Chemistry-Based Force Fields for Poly(ethylene oxide) with Many-Body Polarization Interactions

Oleg Borodin*,† and Grant D. Smith†,‡

Department of Materials Science and Engineering, 122 S. Central Campus Drive, Rm. 304, University of Utah, Salt Lake City, Utah 84112, and Department of Chemical and Fuels Engineering, University of Utah, Salt Lake City, Utah 84112

Received: November 22, 2002; In Final Form: April 14, 2003

A methodology for consistent development of the quantum chemistry-based force fields with and without many-body polarizable terms is described. Adequate levels of theory and basis sets for determination of the relative conformational energetics, repulsion and dispersion nonbonded parameters, dipole moments, and molecular polarizability are established. Good agreement between the quantum chemistry-based repulsion and dispersion parameters and those previously obtained by fitting crystal structures of poly(oxymethylene) is obtained. Hartree−Fock (HF) calculations with augmented correlation consistent basis sets are adequate for the determination of repulsion parameters, whereas a double extrapolation to improved treatments of electron correlations and larger basis sets is needed to obtain dispersion parameters. Partial charges are obtained by fitting to the electrostatic grid of model compounds. Atomic polarizabilities are fitted to reproduce polarization energy around the model compounds. The density functional B3LYP yields relative conformational energies in better agreement with Møller−Plesset second-order (MP2) perturbation theory than the HF energies; however, the accuracy of the B3LYP density functional was insufficient to provide reliable relative conformational energetics. A molecular mechanics study of the conformational energetics of 1,2-dimethoxyethane indicated that many-body polarizable interactions have little impact on the relative conformational energies.

I. Introduction

Poly(ethylene oxide) (PEO) has a wide range of technologically important applications. For example, the grafting of PEO on the surface or adsorption of PEO−poly(propylene oxide)−PEO block copolymers (Pluronic) prevents protein adsorption and denaturation, thus making surfaces more biocompatible.[1−6] Lightly cross-linked PEO is the main constituent of many hydrogels that are used for drug delivery applications.[7] Attaching PEO to proteins prevents them from being adsorbed on surfaces,[3] whereas aqueous solutions of PEO with dextran, starch, and poly(vinyl alcohol) are used for industrial protein partitioning.[3] Solutions of PEO with alkali-metal salts have been widely studied as potential polymer electrolytes.[8] Other important applications of PEO include novel surfactants,[9] modification of natural and artificial membranes,[10,11] and aqueous biphasic separations.[12] In all these applications, PEO interacts with the salts and/or with water, indicating a need for accurate and transferable PEO/water and PEO/salt potentials that can be applied for the study of a broad range of potential applications. Development of an accurate PEO/water potential is described elsewhere,[13] together with the results of molecular dynamics (MD) simulations of PEO in aqueous solutions.[13−22] Here, we present a series of three papers that examine (i) development of the PEO force fields with and without many-body polarization interactions; (ii) validation of the developed force fields in MD simulations on PEO and its oligomers, by comparison with existing and new experimental data; and (iii) force field development and MD simulations for PEO/$LiBF_4$ solutions, where the correct treatment of many-body interactions is important. The mechanism of cation transport in PEO/$LiBF_4$ will be investigated after the structural and transport properties of PEO/$LiBF_4$ are validated against available experimental data.

In the first paper, we present a recipe for developing polymer force fields with and without many-body polarization interactions. PEO is used as an example for force field development. We will focus on establishing adequate levels of theory for determination of the relative conformational energetics, repulsion and dispersion nonbonded parameters, dipole moments, and molecular polarizability from quantum chemistry calculations by comparison with experimental data, where available, or with the most-accurate and most-feasible quantum chemistry calculations. The developed force fields will be used to investigate the effect of MB polarization interactions on relative conformational energetics.

II. Current PEO Force Fields

Several nonpolarizable PEO force fields have been employed in MD simulations of PEO, its oligomers, and PEO-based polymer electrolytes.[23−29] None of these models included many-body polarizable interactions in a consistent way. The nonbonded parameters used in the PEO force fields were taken from fitting crystal structures or generic force fields, with an exception of the work by Halley et al.,[23] where ab initio quantum chemistry-based nonbonded parameters were used. The torsional parameters in the PEO force fields were usually obtained by fitting ab initio quantum chemistry calculations at various levels

* Author to whom correspondence should be addressed. E-mail: Oleg.Borodin@eng.utah.edu.
† Department of Materials Science and Engineering.
‡ Department of Chemical and Fuels Engineering.

10.1021/jp027537e CCC: $25.00
Published on Web 06/24/2003

TABLE 1: Relative Conformational Energies of the Most-Important Dimethoxyethane (DME) Conformers from Quantum Chemistry Calculations and the Following Force Fields: Many-Body (MB) Force Fields FF-1, FF-2, and FF-3 and the Two-Body (TB) FF-1 Force Field

energy level of theory[a]	MP2/D95+(2df,p)	MP2/Dz	MP2/Dz	MP2/Dz	MP2/Tz	force fields FF-1 MB, (FF-1 TB), FF-2 MB, FF-3 MB	B3LYP/Dz	HF/Dz
geometry level of theory[a]	HF/D95**	HF/Dz	B3LYP/Dz	MP2/Dz	MP2/Dz		B3LYP/Dz	HF/Dz
				Relative Conformational Energy (kcal/mol)				
ttt	0	0.00	0.0	0.00	**0.00**	0.00, (0.0),0.0,0.0	0	0.00
tgt	0.14	0.16	0.18	0.15	**0.21**	0.16 (0.20),0.19, 0.21	0.19	0.92
tg^+g^-	0.23	0.35	0.24	0.19	**0.39**	0.38 (0.37),0.41, 0.46	0.74	1.66
ttg	1.43	1.35	1.28	1.26	**1.41**	1.24 (1.17),1.22, 1.53	1.54	1.85
tgg	1.51	1.47	1.44	1.27	**1.52**	1.41 (1.40),1.49, 1.46	1.73	2.80
ggg	1.64	1.55	1.54	1.20	**1.60**	2.00 (1.85) 2.23, 2.10	2.57	3.79

[a] The aug-cc-pvDz and aug-cc-pvTz basis sets are denoted as Dz and Tz, respectively.

or were taken from previous force fields: Smith et al.[24] used MP2/D95+(2df,p)//HF/D95** dimethoxyethane (DME) energetics, whereas Neyertz et al.[25] used the MP2/6-311++G**//HF/3-21G diglyme energetics. Halley at el.[26] used a torsional potential from previous work that predicted the energetics of the major conformers within 0.5 kcal/mol from the MP2/D95+(2df,p)//HF/D95** DME quantum chemistry data of Smith et al.,[24] with the tg^+g^- conformer being 1.6 kcal/mol below the quantum chemistry values. Müller-Plathe and co-workers[27,28] modified the empirical potential to reproduce the gauche effect, whereas the AMBER force field was used by the Wheeler group without any validation.[29]

III. Quantum Chemistry Calculations

A. Conformational Energetics and Geometries. Structural properties of polymers, such as the characteristic ratio, are crucially dependent on the relative conformational energies and conformational geometries, whereas accurate representation of the barriers between the most important conformers is important for realistic representation of polymer dynamics. Therefore, conformational properties are central to the investigation of the influence of chemical structure on polymer dynamic and structural properties. Conformational characteristics of 1,2-dimethoxyethane (DME) as a model compound for PEO have been investigated for the last 40 years, because of the differences between the crystal-, liquid-, and gas-phase conformations. Analysis of IR and Raman spectra indicate that the −C−C− bonds adopt gauche (g) conformation in the crystal phase,[30] whereas a mixture of trans (t) and g conformers is observed in the gas and liquid phases.[31−33] In an IR study of DME that was trapped in an argon matrix, Yoshida et al.[31] suggested that the ttt conformer around the −O−C−C−O− bonds is the most stable. A subsequent IR study of gaseous DME under reduced pressure allowed the authors to estimate the tg^+g^- (tg^-g^+) energy to be 0.31 (±0.04) kcal/mol, relative to the ttt conformer, from the ratio of the adsorption peaks.[33] Analysis of NMR vicinal coupling constants of DME in the gas phase indicated a trans fraction of ∼0.25 around the −C−C− bond at 130−170 °C.[33] Electron diffraction experiments[34] indicated that the energy difference between the ttt and tgg or tg^+g^- conformers is small, which leads to a large population of tg^+g^- or tgg conformers, along with ttt conformers, in the gas phase.

Several ab initio quantum chemistry studies of DME have been reported.[35−37] The effect of basis set size and the importance of correlation effects have been investigated by studying the energy difference between the tgt and ttt conformers. Inclusion of the electron correlation effect, using Møller−Plesset second-order perturbation theory (MP2), reduced the tgt energy by 0.6−1.1 kcal/mol.[37] Inclusion of the third-order perturbations (MP3) increased the tgt energy by ∼0.2−0.25 kcal/mol, whereas inclusion of the fourth-order (MP4) terms results in a reduction of the tgt energy, by 0.1 kcal/mol, relative to the MP3 energies.[36] Coupled-cluster calculations that included single and double excitations (ΔCCSD) yielded energies that were similar to the MP4 energies. Inclusion of triple excitations (ΔCCSD(T)) reduced the energy by ∼0.1 kcal/mol for the largest basis sets investigated (6-311+G**), bringing the ΔCCSD(T) energies within 0.1 kcal/mol of the MP2 energies for the 6-311G*−6-311+G** basis sets and suggesting that, for a large basis set, inclusion of the electron correlation beyond the MP2 level had an insignificant effect on the conformational energy of tgt (relative to ttt).[37] Jaffe, Smith, and co-workers[37] have extensively investigated the effect of basis set size on the tgt conformational energy. They have found that inclusion of the first set of diffuse functions into the D95** and 6-311G** basis sets reduced the gauche energy by 0.23−0.35 kcal/mol at the MP2 or CCSD(T) levels, whereas additional sets of diffuse sp-functions did not have much effect on the gauche energy. They also found that it was important to include polarization functions beyond the minimum representation. It was concluded that the MP2/D95+(2df,p)//HF/D95** level was capable of predicting DME conformational energies within an accuracy of 0.2−0.3 kcal/mol.

The conformational energetics for all DME conformers was calculated at the MP2/D95+(2df,p)//HF/D95** level.[37] Table 1 lists only the lowest-energy conformers. Abe et al.,[38] after careful comparison of the existing RIS models against available experimental data, concluded that the RIS model that is based on MP2/D95+(2df,p)//HF/D95** conformational energies provided a reasonable depiction of DME in the gas phase. Conformational populations obtained at the MP2/D95+(2df,p)//HF/D95** level also were found to be in good agreement with the electron diffraction data.[34]

Despite the MP2/D95+(2df,p)//HF/D95** level conformational energetics being successful in reproducing electron diffraction data, NMR vicinal coupling data,[37,38] and tg^+g^- conformer energy from IR spectra, we wish to continue ab initio studies of DME conformational energetics, to answer three additional questions: (a) What is the influence of the level of theory (HF, MP2, density functional theory (DFT) methods) that is used in geometry optimization on the conformational energetics? (b) Does an additional significant increase of the basis-set size and augmentations change the relative conformational energetics of DME at the MP2 level? (c) Are much less computationally expensive DFT methods capable of adequately predicting the conformational energies of DME, when compared to MP2 methods?

We have chosen augmented correlation consistent polarized valence basis sets (aug-cc-pvXz, where X = D (T for double-ζ basis sets) or T (for triple-ζ basis sets))[39] for our further quantum

TABLE 2: Backbone Torsional Angles for the Most-Important DME Conformers, Calculated Using the aug-cc-pv-Dz Basis Set at the HF, MP2 Levels of Theory and Using the B3LYP Density Functional[a]

level of theory, FF	Backbone Torsional Angle (degrees) ϕ_1	ϕ_2	ϕ_3
	ttt Conformer		
all	180.0, 180.0, **180.0**	180.0, 180.0, **180.0**	180.0, 180.0, **180.0**
	tgt Conformer		
HF, B3LYP, **MP2**	184.1, 183.4, **183.8**	72.2, 74.7, **72.8**	184.1, 183.4, **183.8**
FF-1, FF-2, FF-3 MB	183.0, 183.1, 186.3	68.4, 68.5, 67.3	183.0, 183.1, 186.3
FF-1 TB	183.0	68.8	183.0
	tgg Conformer		
HF, B3LYP, **MP2**	180.7, 181.0, **179.8**	65.0, 67.5, **58.5**	75.9, 74.8, **59.9**
FF-1, FF-2, FF-3 MB	181.1, 181.3, 181.7	60.0, 59.6, 56.0	69.2, 70.2, 58.0
FF-1 TB	180.8	59.3	68.3
	tg^+g^- Conformer		
HF, B3LYP, **MP2**	182.1, 180.6, **180.7**	71.7, 76.6, **75.1**	268.2, 274.6, **278.8**
FF-1, FF-2, FF-3 MB	181.5, 181.8, 182.5	81.7, 82.3, 87.0	288.2, 287.3, 293.1
FF-1 TB	181.5	82.2	288.5
	ttg Conformer		
HF, B3LYP, **MP2**	181.7, 181.4, **180.8**	179.3, 179.7, **178.7**	89.3, 83.0, **81.2**
FF-1, FF-2, FF-3 MB	181.2, 181.1, 182.0	168.8, 166.8, 168.2	78.5, 78.3, 71.7
FF-1 TB	181.5	168.5	77.5
	ggg Conformer		
HF, B3LYP, **MP2**	64.3, 63.9, **58.1**	49.9, 51.4, **45.6**	64.0, 63.9, **58.1**
FF-1, FF-2, FF-3 MB	63.8, 63.4, 56.9	50.0, 50.4, 49.7	63.8, 63.4, 56.9
FF-1 TB	63.2	50.6	63.2

[a] Geometries for the following force fields are also given: many-body (MB) force fields FF-1, FF-2, and FF-3; two-body (TB) force field FF-1.

chemistry studies that are performed with the Gaussian 98 package.[40] These basis sets are constructed by grouping together all the functions that reduce the atomic correlation energy by the same amount and then adding these groups to the atomic Hartree−Fock (HF) orbitals. Thus, for a given accuracy in the correlation energy, these sets are as compact as possible. The conformational energetics of the most important DME conformers were calculated at the MP2/aug-cc-pvDz//HF/aug-cc-pvDz level and are compared in Table 1 with the previous energies that were obtained at the MP2/D95+(2df,p)//HF/D95** level. The relative energies for the tg^+g^- and ttt conformers at the MP2/aug-cc-pvDz//HF/aug-cc-pvDz level differ from those at the MP2/D95+(2df,p)//HF/D95** level by ∼0.1 kcal/mol, whereas the relative energies of the other most important conformers (tgt, tgg, ggg, ttg) differ by less than 0.04 kcal/mol. The similarity of the MP2/aug-cc-pvDz//HF/aug-cc-pvDz and MP2/D95+(2df,p)//HF/D95** energies is expected, because the aug-cc-pvDz and D95+(2df,p) basis sets are similar in size, containing 236 and 228 basis functions, respectively.

We proceed by investigating the effect of the level of theory on the geometries (dihedral angles) of the most-important conformers. Torsional angles for the most-important DME conformers are summarized in Table 2 for the MP2, HF, and B3LYP[41] calculations, using the aug-cc-pvDz basis set. Torsional angles of the tgt conformer are within 2° for all levels of theory, whereas more-significant deviations were seen for the other conformers. The HF level yields torsional angles that differ by up to 10°−15° from the MP2 torsional angles for the tgg and tg^+g^- conformers. In general, the B3LYP DFT calculations yield dihedral angles that are more similar to those from the MP2 calculations than those from the HF calculations.

The energies of DME conformers that have been calculated for the MP2, HF, and B3LYP geometries, using the MP2/aug-cc-pvDz single-point energy calculations, are presented in Table 1. The tgt energy for the HF and MP2 geometries are almost identical, whereas the energies for the other conformers differ by 0.1−0.35 kcal/mol, with the effect being the largest for the ggg conformer. The conformational energies that have been calculated at the MP2/aug-cc-pvDz level, using the B3LYP geometries, tend to agree better with those calculated at the MP2 geometries than the conformational energies that are calculated using the HF geometries. The average deviation of the backbone DME dihedral angles of the B3LYP/aug-cc-pvDz geometry from those for the MP2/aug-cc-pvDz geometry is 3.6°, which is slightly better than the average deviation of the DME backbone dihedrals at HF/aug-cc-pvDz from the MP2/aug-cc-pvDz level (4.4°), which suggests that it is preferential to use the B3LYP geometries rather than the HF geometries if the MP2 geometries are too expensive to compute.

Given the increase in computer speed over the past decade, it is now feasible to perform calculations at the MP2 level with much larger basis sets than with the D95+(2df,p) basis set that was used in the previous study of DME in 1993.[37] The conformational energetics of DME were calculated at the MP2/aug-cc-pvTz level for MP2/aug-cc-pvDz geometries and are presented in Table 1. The increase of the basis-set size from the aug-cc-pvDz to aug-cc-pvTz for the MP2/aug-cc-pvDz geometries increases the conformational energy of tgt only by 0.06 kcal/mol; the energies of the tg^+g^-, ttg, and tgg conformers are increased by 0.15−0.25 kcal/mol, whereas a significant increase in the ggg conformational energy by 0.4 kcal/mol is also observed.

The correlation energy (MP2−HF) of the DME conformers is summarized in Table 3. The ggg conformer has the largest correlation contribution (∼2.9 kcal/mol) to the relative conformational energy, whereas the tgg and tg^+g^- conformers have the second-largest correlation contribution, ∼1.6−1.7 kcal/mol. The large correlation energy of these conformers is responsible for the largest deviations of the HF geometries from the MP2 geometries for these conformers. The smallest correlation contribution for the ttg and tgt conformers, on the other hand, results in the smallest differences between the HF and MP2 geometries. It is also interesting that the correlation energy contribution to the relative conformational energies is weakly dependent on the basis-set size (triple-ζ versus double-ζ) and

TABLE 3: Correlation Contribution[a] to the Relative Conformational Energy for the Most-Important DME Conformer, Calculated Using the MP2/aug-cc-pvDz Geometries

	Correlation Contribution (kcal/mol)	
conformer	(MP2−HF)/aug-cc-pvDz	(MP2−HF)/aug-cc-pvTz
ttt	0.0	0
tgt	−0.78	−0.72
tg^+g^-	−1.64	−1.63
ttg	−0.69	−0.67
tgg	−1.81	−1.71
ggg	−2.98	−2.93

[a] The correlation contribution is defined as MP2 energy − HF energy.

is <0.02 kcal/mol for the ttg and tg^+g^- conformers (<0.1 kcal/mol for the other conformers).

The next issue that we address is the ability of the density functional theory (DFT) to predict conformational energetics. Yoshida and Matsuura[35] performed DFT and ab initio quantum chemistry calculation of the DME conformers at the 6-31G* level and found that the B3LYP functional yielded a conformational energy of 0.31 kcal/mol for the tg^+g^- conformer, which is in good agreement with the estimates from IR experiments,[33] whereas the B3LYP energy of 0.51 kcal/mol for the tgt conformer agreed nicely with the MP3/6-311+G*//HF6-311+G* energy of 0.51 kcal/mol. These results suggest that the B3LYP functional is able to provide reliable conformational energetics for DME. To check this supposition, we calculated the conformational energetics of DME using the same B3LYP functional with the much larger aug-cc-pvDz basis set, compared to the 6-31+G* basis set that was used by Yoshida and Matsuura.[35] Table 1 indicates that the B3LYP energy for the tg^+g^- conformer with the aug-cc-pvDz basis set is 0.74 kcal/mol, which is 0.4 kcal/mol higher than the B3LYP/6-31+G* energy. This indicates that the good agreement between the B3LYP/6-31+G* energy of the tg^+g^- conformer (0.31 kcal/mol) and the experimental value of 0.31 kcal/mol and our best estimate of 0.39 kcal/mol is serendipitous and is caused by the cancellation of errors that are due to basis-set incompleteness and deficiencies in the B3LYP density functional. The B3LYP/aug-cc-pvDz energy of the ggg conformer is also off by ∼1 kcal/mol from our best estimate, whereas the energy of the tgt conformer is predicted within 0.05 kcal/mol of our best estimate. After comparing the HF, MP2, and B3LYP energies for the most-important DME conformers, we conclude that, despite the B3LYP energies being in better agreement with the MP2 energies, compared to the HF energies, they are still unreliable (causing errors up to 1 kcal/mol in conformational energies) and, therefore, should not be used for parametrization of the potential energy function, which requires accuracies of 0.2 kcal/mol for the relative energies of the most-important conformers. However, the B3LYP functional, even with a small 6-31+G* basis set, yielded vibrational frequencies that were in excellent agreement with the experiment after uniform scaling by a factor of 0.97,[35] indicating that a set of reliable force constants could be obtained at the B3LYP/6-31+G* level.

The MP2/aug-cc-pvTz//MP2/aug-cc-pvDz energies are our best estimate, and we believe that a further increase in basis-set size will change the conformational energetics by <0.1 kcal/mol for the most-important DME conformers. We estimate the uncertainty in the energies due to incomplete treatment of electron correlation to be 0.1 kcal/mol and the uncertainty due to neglect of zero-point energies and thermal-vibrational contributions to be 0.1 kcal/mol. We expect that the use of the conformer geometries obtained at the level higher than MP2/aug-cc-pvDz will make a difference of <0.1 kcal/mol. Therefore, the uncertainty of the relative conformer energies obtained at the MP2/aug-cc-pvTz//MP2/aug-cc-pvDz level is 0.3 kcal/mol or even less, because of the cancellation of errors that are introduced by various approximations. In fact, because of error cancellation, the DME conformational energies at the MP2/aug-cc-pvTz//MP2/aug-cc-pvDz level are within 0.16 kcal/mol of the previous calculations, using a much smaller basis set and the HF geometries (MP2/D95+(2df,p)//HF/D95**), with an absolute average deviation of only 0.06 kcal/mol.

B. Dipole Moment and Polarizability. Electrostatic interactions such as coulomb and polarization interactions yield a major contribution to the PEO−cation complexation energy and a significant contribution of the PEO−water binding,[13] indicating that care must be taken to use an adequate level of theory and a basis set to ensure accurate prediction of the electrostatic potential, dipole moments, and polarizability from quantum chemistry during force field parametrization.

Dipole moment and dipole polarizability of a dimethyl ether are known from experimental studies;[42] therefore, we investigate the effect of basis set and level of theory on the ability of quantum chemistry calculations to represent these properties of dimethyl ether. The results of this investigation are presented in Table 4. Commonly used small basis sets such as 6-31+G* overestimate the dimethyl ether dipole moment by 12%−17%, whereas its polarizability is underestimated by 16%−25%. The B3LYP density functional yields the dipole moment and polarizabilities in best agreement with experimental data. A basis set increase from the split-valence double-ζ to split-valence triple-ζ results in marginal changes of the dipole moment and polarizabilities. The addition of a set of d- and f-polarization functions on heavy atoms and a set of p-functions on hydrogen atoms decreases the dipole moment by 4%−10% and brings it within 8% of the experimental values, whereas the dipole polarizability improves only by 0.2 $Å^3$. The D95+(2df,p) basis set yields results that are similar to those of the 6-311+G(2df,p) basis set. The aug-cc-pvDz basis set, however, yields results that best agree with the experimental values. Increasing the basis set size to aug-cc-pvTz does not result in a significant improvement of the dipole moment and polarizability, whereas the removal of the augmentation leads to significant underestimation of the polarizability for all levels of theory and significant underestimation of dipole moment at the B3LYP level.

In summary, the B3LYP functional is able to predict the dimethyl ether dipole moment and polarizability accurately within the limits of the atomic basis sets that were employed. Ability of the HF levels to predict the dimethyl ether dipole moment is comparable to that of the MP2 level and is worse than that for B3LYP. Predictions of the dipole polarizability was always in the following order for the basis sets investigated: HF < MP2 < B3LYP. The B3LYP/aug-cc-pvDz level is the most accurate for combined prediction of the dipole moment (electrostatic potential) and polarizability and, therefore, is used in the future studies of the electrical properties of PEO oligomers.

The dipole moment and dipole polarizability were calculated for the most-important DME conformers and are summarized in Table 5. The ttt conformer has a zero dipole moment, because the dipole moments of the monomers are antiparallel. The tgg conformer has the largest dipole moment. The dipole moments of the other most important conformers are significant, ranging from 1.37 to 1.63 D, suggesting that we can expect strong electrostatic interactions of PEO with ions and polar liquids such as water. The B3LYP/aug-cc-pvDz level yields DME dipole moments ∼5%−20% lower than the HF/D95+(2df,p)//HF/

TABLE 4: Dipole Moment and Dipolar Polarizability of Dimethyl Ether as a Function of the Basis Set and Level of Theory

		Dipole Moment (D)			Polarizability (Å^3)		
basis set	basis function	HF	MP2	B3LYP	HF	MP2	B3LYP
6-31+G*	69	1.53	1.61	1.46	3.96	4.27	4.44
6-311G*	72	1.44	1.38	1.29	3.81	4.03	4.19
6-311+G*	84	1.53	1.56	1.45	4.04	4.36	4.51
6-311+G(2df,p)	138	1.40	1.41	1.33	4.28	4.56	4.74
D95+(2df,p)	129	1.41	1.43	1.36	4.20	4.47	4.68
cc-pvDz	72	1.37	1.24	1.14	3.87	4.07	4.21
aug-cc-pvDz	123	1.37	1.36	1.27	4.60	5.01	5.14
aug-cc-pvDz[b]	123	1.51	1.36	1.32	4.71	5.01	5.15
aug-cc-pvTz[b]	276	1.51		1.32	4.73		5.17
experiment[c]			1.3 (±0.01)			5.29[d]	

[a] The geometry optimization was performed at the level of theory corresponding to that used in the dipole moment and polarizability calculations, unless specified otherwise. [b] MP2/aug-cc-pvDz geometry was used. [c] From ref 42. [d] An uncertainty of 0.3%−8% was reported for this data compilation.

TABLE 5: Molecular Dipole Moment and Polarizability of the Most-Important DME Conformers from Quantum Chemistry Calculations and Force Fields

single-point calculation set	HF/D95+(2df,p)	B3LYP/aug-cc-pvDz	force fields with no weighting, ϕ-weighting (FF-1), and ϕ^2-weighting (FF-2 and FF-3)
geometry	HF/D95**	B3LYP/aug-cc-pvDz	
		Dipole Moment (D)	
ttt	0.0	0.0	0.0, 0.0, 0.0
tgt	1.52	1.37	1.42, 1.60, 1.61
tg^+g^-	1.65	1.52	1.59, 1.76, 1.80
ttg	1.93	1.63	1.57,1.74, 1.77
tgg	2.67	2.39	2.37, 2.64, 2.67
ggg	1.49	1.41	1.51, 1.67, 1.71
		Polarizability (Å^3)	
ttt		9.30	9.98
tgt		9.84	10.2
tg^+g^-		9.55	10.4
ttg		9.43	10.3
tgg		9.46	10.4
ggg		9.14	10.4

[a] Dipole moments from the three force fields presented below correspond to the fits to the electrostatic potential, using the following objective functions: (a) $\sum(\phi_i^{QC} - \phi_i^{FF})^2$, or no weighting function; (b) $\sum|\phi_i^{QC}|(\phi_i^{QC} - \phi_i^{FF})^2$, or the absolute value of the electrostatic potential (ϕ-weighting) used in the FF-1 force field; and (c) $\sum(\phi_i^{QC})^2(\phi_i^{QC} - \phi_i^{FF})^2$ objective function, or the ϕ^2-weighting used in the FF-2 and FF-3 force fields.

D95** level,[37] in accord with the aforementioned investigation of the basis set and a level of theory on the dimethyl ether dipole moment. Polarizability for the most-important DME conformers was calculated at the B3LYP/aug-cc-pvDz level and is summarized at Table 5. The polarizability variation of <10% between all conformers indicates that the DME polarizability is only weakly dependent on the DME geometry. It is also only slightly less than the polarizability of two noninteracting dimethyl ethers of 10.3 Å^3 at the B3LYP/aug-cc-pvDz level, suggesting that the polarizability is approximately additive on the monomer (i.e., dimethyl ether) length scale.

IV. Force Field Development

A. Force Field Development Methodology. In the classical force field developed below, the total potential energy of the ensemble of atoms, represented by the coordinate vector $\boldsymbol{r}$, is denoted as $U^{tot}(\boldsymbol{r})$. The latter is represented as a sum of nonbonded interactions ($U^{NB}(r_{ij})$) as well as energy contributions due to bonds that have a bond length r_{ij} ($U^{BOND}(r_{ij})$), bends that have a bending angle θ_{ijk} ($U^{BEND}(\theta_{ijk})$), and dihedrals with a dihedral angle ϕ_{ijkl} ($U^{TORS}(\phi_{ijkl})$), and is given by eq 1:

$$U^{tot}(\boldsymbol{r}) = U^{NB}(\boldsymbol{r}) + \sum_{ij} U^{BOND}(r_{ij}) + \sum_{ijk} U^{BEND}(\theta_{ijk}) + \sum_{ijkl} U^{TORS}(\theta_{ijkl}) \quad (1)$$

The nonbonded energy $\boldsymbol{U}^{NB}(\boldsymbol{r})$ (eq 2) consists of a sum of the two-body repulsion and dispersion energy terms between atoms i and j and is represented by the Buckingham (exp-6) potential, the energy due to charge−charge interactions (coulombic), and a potential energy due to dipole many-body polarization U^{pol}:

$$U^{NB}(\boldsymbol{r}) = \frac{1}{2}\left[\sum_i \sum_j A_{ij} \exp(-B_{ij} r_{ij}) - \frac{C_{ij}}{r_{ij}^6} + \frac{q_i q_j}{4\pi\epsilon_0 r_{ij}}\right] + U^{pol}(\boldsymbol{r}) \quad (2)$$

The potential energy due to dipole polarization is not pairwise additive and is given by a sum of the interaction energy between the induced dipoles (μ_i) and the electric field E_i^0 at atom i generated by the permanent charges in the system (the first term in eq 3), the interaction energy between the induced dipoles (the second term in eq 3), and the energy required to induce the dipole moments μ_i (the third term in eq 3):[43]

$$U^{pol}(\boldsymbol{r}) = -\sum_i \mu_i \cdot \boldsymbol{E}_i^0 - 0.5 \sum_i \sum_j \mu_i \cdot \boldsymbol{T} \cdot \mu_j + \sum_i \left(\frac{\mu_i \cdot \mu_i}{2\alpha_i}\right) \quad (3)$$

where $\mu_i = \alpha_i E_{tot}$, α_i is the isotropic atomic polarizability, E_{tot} is the total electrostatic field at the atomic site i due to permanent

charges and induced dipoles, and the second-order dipole tensor $\boldsymbol{T_{ij}}$ is given by

$$\boldsymbol{T_{ij}} = \nabla_i \nabla_j \frac{1}{4\pi\epsilon_0 r_{ij}} = \frac{1}{4\pi\epsilon_0 {r_{ij}}^3}\left(\frac{3\boldsymbol{r_{ij}}\boldsymbol{r_{ij}}}{{r_{ij}}^2} - 1\right) \quad (4)$$

The nonbonded contributions including the potential energy due to polarization were calculated for all intermolecular atom pairs (*ij*) and for the intramolecular atom pairs that were separated by more than two bonds.

The contributions due to bonds $U^{\mathrm{BOND}}(r_{ij})$, bends $U^{\mathrm{BEND}}(\theta_{ijk})$, and torsions $U^{\mathrm{TORS}}(\phi_{ijkl})$ for atoms *i*, *j*, *k*, and *l* are given by eqs 5−7:

$$U^{\mathrm{BOND}}(r_{ij}) = \frac{1}{2} {k_{ij}}^{\mathrm{BOND}} (r_{ij} - {r_{ij}}^0)^2 \quad (5)$$

$$U^{\mathrm{BEND}}(\theta_{ijk}) = \frac{1}{2} {k_{ijk}}^{\mathrm{BEND}} (\theta_{ijk} - {\theta_{ijk}}^0)^2 \quad (6)$$

$$U^{\mathrm{TORS}}(\phi_{ijkl}) = \sum_n \frac{1}{2} {k^{\mathrm{t}}}_{ijkl}(n)[1 - \cos(n\phi_{ijkl})] \quad (7)$$

where ${r_{ij}}^0$ is an equilibrium bond length, ${\theta_{ijk}}^0$ is an equilibrium bend angle, and ϕ_{ijkl} is a dihedral. The terms ${k_{ij}}^{\mathrm{BOND}}$, ${k_{ijk}}^{\mathrm{BEND}}$, and ${k^{\mathrm{t}}}_{ijkl}(n)$ are the bond force constants, bend force constants, and torsional parameters. Nonbonded interactions including many-body polarization terms are evaluated for all intermolecular atom pairs (*ij*) and for intramolecular atom pairs that are separated by three or more bonds.

We adopt the following methodology for the many-body (MB) polarizable force field development. The atomic polarizability is obtained by fitting polarization energies around DME. The partial charges are obtained by fitting electrostatic grid around the ethylene oxide oligomers. A suitable set of the repulsion and dispersion parameters then is determined. Bond and bend force constants could be obtained by fitting frequencies of the model compounds; however, in this work, we simply used the parameters from the previous MD simulations of the nonpolarizable PEO.[24] Next, the equilibrium bond length and bend angles (eqs 5 and 6) are fitted to obtain the best representation of the conformational geometries, and the torsional parameters (eq 7) are fitted to obtain the best representation of the conformational energetics of DME.

B. Partial Charges and Atomic Polarizabilities. In our model, which includes the many-body induced dipole polarizability energy, the electrostatic potential around a molecule is no longer only a function of partial charges. Indeed, the partial charges on the atoms separated by more than three bonds from a given polarizable atom create an electric field at that atom, resulting in an induction of an atomic dipole moment, which contributes to the electrostatic field around the molecule and should be considered during partial charge fitting. Thus, the atomic polarizabilities are required before fitting partial charges.

The molecular dipole polarizability of DME and dimethyl ether calculated at the B3LYP/aug-cc-pvDz level is given in Tables 4 and 5. Allinger's group[44] and Dykstra's group[45] both suggested that the interaction between induced dipoles has a minor effect on molecular polarizability, and a sum of atomic polarizabilities could be used to approximate the molecular polarizability tensor with an average error of 10% and the isotropic polarizability with an average error of 3%.[45] Our observation of molecular dipole polarizability of the most-important DME compounds being the same (within 10%) also suggests that interaction between the induced dipoles is small. Because of weak interaction between the atomic polarizabilities,

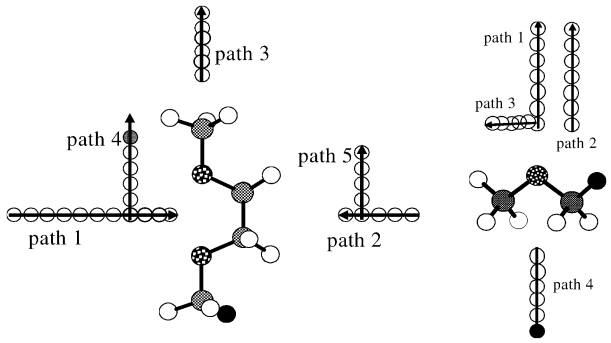

Figure 1. Paths for calculation of the electrostatic potential and polarization energy around the tgt conformer of DME and the dimethyl ether.

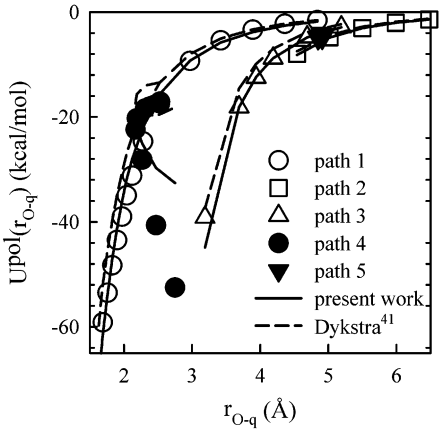

Figure 2. Polarization energy as a function of ether oxygen (EO) charge separation (r_{O-q}) along paths 1−5 around the tgt conformer from the B3LYP/aug-cc-pvDz quantum chemistry calculations (symbols), from Dykstra's model[45] (dashed lines), and from the fit to polarization energy around a molecule (force field) (solid lines).

one cannot use the molecular polarizability tensor to partition molecular polarizability into the atomic polarizabilities. However, a least-squares fit of the atomic polarizabilities to molecular polarizability for a large set of compounds allows partitioning of molecular polarizability to its atomic contributions. Dykstra's group reported values of the following isotropic polarizabilities from such a fit: $\alpha_{C(sp3)} = 1.874$ Å^3 and $\alpha_{-O-} = 0.748$ Å^3 with the hydrogen polarizability included into the polarizabilities of the heavy atom.[45] Summation of the atomic polarizabilities yields molecular polarizabilities of 4.5 Å^3 for dimethyl ether and 9.0 Å^3 for DME, ∼10%−20% below the quantum chemistry values of 5.1 Å^3 and 9.1−9.8 Å^3 for dimethyl ether and DME, respectively, as reported in Tables 4 and 5. We wish to investigate the ability of these polarizabilies to represent the polarization energy due to a unit charge (+1 e) around a DME-(tgt) molecule along the paths shown in Figure 1, because this polarization energy is expected to contribute significantly to the Li^+ or another cation complexation energy with PEO and DME. The polarization energy is calculated as the energy of the DME with the (+1 e) charge, minus the self-energy of DME at the same geometry, minus the electrostatic potential at the point location of the unit charge. Figure 2 demonstrates that polarizabilities from ref 45 significantly underestimate polarization energy along paths 1, 3, and 4. For example, for the most probable Li^+ position $r(O-q) = 2.4$ Å along path 1, Dykstra's model yields a polarization energy of −27.1 kcal/mol, whereas the B3LYP/aug-cc-pvDz level quantum chemistry yields a value of −34.9 kcal/mol, indicating an underestimation, by >20%, of the polarization energy by the model.

TABLE 6: Charges and Polarizabilities for the PEO Force Field

atom	polarizability (Å^3)	charge (e) for FF-1 force field[a]	charge (e) for FF-2 and FF-3 force fields[b]
C_m[c]	1.67	0.0200	−0.1187
C_e[d]	1.40	0.0661	−0.0326
O	1.13	−0.3166	−0.2792
H	0.18	0.0461	0.0861

[a] From the electrostatic potential fit, using the absolute value of the electrostatic potential (ϕ-weighting) and the following WDR radii: $r^{VDW}(O) = 1.7$ Å, $r^{VDW}(H) = 1.8$ Å, and $r^{VDW}(C) = 2.1$ Å. [b] From the electrostatic potential fit, using the square of the electrostatic potential (ϕ^2-weighting) and the following WDR radii: $r^{VDW}(O) = 2.0$ Å, $r^{VDW}(H) = 1.8$ Å, and $r^{VDW}(C) = 2.5$ Å. [c] C_m denotes a methyl carbon of the CH_3 group. [d] C_e denotes all other carbon atoms.

To obtain an improved description of the polarization energy around the most-important PEO oligomers, we suggest partitioning the atomic polarizabilities by fitting the polarizable energy around a molecule obtained at the B3LYP/aug-cc-pvDz level quantum chemistry calculations. The atomic polarizabilities of similar atoms types were constrained to be equal during the fit. The ability of the atomic polarizable dipoles from the fit to reproduce polarization contribution to the potential energy is shown in Figure 2. This figure also indicates that the isotropic dipole polarizabilities from the fit are better able to represent polarization energy around DME than atomic polarizabilities from Dykstra's model[45] and, therefore, will be used for modeling MB polarization effects in PEO and PEO/salt systems. The values of the atomic polarizabilities from the current fit are shown in Table 6. The molecular polarizability tensor was calculated using these atomic polarizabilities. The trace of the molecular polarizability tensor from quantum chemistry calculations is compared with that from the force field in Table 5. The force field yields a molecular polarizability that is, on average, 8% higher than the quantum chemistry values. Indeed, the atomic polarizabilities in the force field are fitted to reproduce the total polarization energy, not just dipole polarization, and, therefore, are representing the "effective" atom dipole polarizabilities that effectively include higher-order polarizabilities, whereas the molecular dipole polarizability from quantum chemistry does not incorporate hyperpolarizabilities. Therefore, the force field molecular polarizability is expected to be slightly higher than the quantum chemistry values.

At the next stage of the force field development, we determine partial charges by fitting an electrostatic grid around a dimethyl ether molecule, five conformers of DME (ttt, tgt, ttg, tgg, ggg) and the tttttt conformer of diglyme. During the fit, the mean-square deviation of the force field electrostatic potential from that obtained by the B3LYP/aug-cc-pvDz level was minimized. Following Breneman and Wiberg,[46] we exclude electrostatic potential grid points inside molecular van der Waals (VDW) radii from the fit, because the approach of any atom inside the VDW radii is highly unlikely in MD simulations. Previous MD simulations of PEO melts, PEO/LiI,[47] and PEO/$LiPF_6$[48] were used to define the VDW radii. The oxygen atom VDW radius, $r^{VDW}(O) = 1.75 \pm 0.1$ Å, was based on the closest approach of the Li^+ cation to an ether oxygen (EO) atom from the $g^{OLi}(r)$ radial distribution function (RDF) for the PEO/Li salts MD simulations; the hydrogen VDW radius, $r^{VDW}(H) = 1.8 \pm 0.15$ Å, was based on $g^{HH}(r)$, $g^{HO}(r)$, and $g^{HF}(r)$ RDFs, whereas $r^{VDW}(C) = 2.2 \pm 0.2$ Å was based on $g^{CLi}(r)$, $g^{CLi}(r)$, and $g^{CF}(r)$. Electrostatic grid points that were more than 3.5 Å away from any atom were also excluded from the fit, to obtain a relatively homogeneous layer of electrostatic grid points around a molecule. In the initial fit, all points around the DME and diglyme molecules were weighted equally; i.e., no position-dependent weighting was used. The partial charges from this fit are given in Table 6. The dipole moments of the most-important DME conformers calculated using the resulting charges are shown in Table 5, indicating good agreement between the force field and quantum chemistry values. The mean-square average deviation of the force field electrostatic potential from the quantum chemistry electrostatic potential was 0.7−1.2 kcal/mol, also indicating that the partial charges can reproduce electrostatic potential around DME and diglyme molecules well.

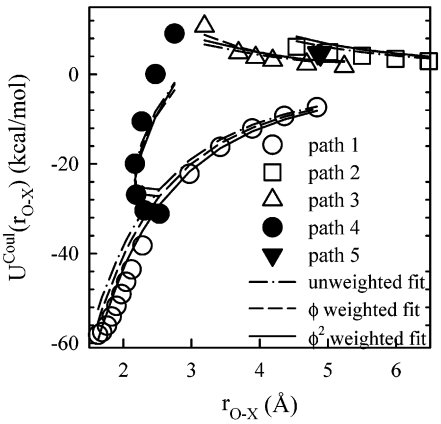

Figure 3. Electrostatic potential as a function of the separation from the EO atom (r) around the tgt conformer from quantum chemistry and three fits to the electrostatic potential (a) without weighting, (b) using the absolute value of the electrostatic potential (ϕ-weighting), and (c) with ϕ^2-weighting.

A closer examination of the electrostatic potential along paths 1 and 4 around the tgt conformer shown in Figure 3 indicates that the force field severely (∼10 kcal/mol) underestimates the electrostatic potential in the proximity of the EO atoms ($r(O-q) \approx 2.0$ Å), where the strongest binding of the Li^+ cation is expected.[47] This underestimation occurs because the number of points farther from the atom scales as a square of the distance, resulting in more atoms being included in the fit at longer distances, effectively giving larger weight to the more-distant points in the electrostatic potential ϕ_i^{QC} fit. To increase the contribution to the objective function from the points in the proximity of the oxygen atom during the partial charge fitting, we examined two approaches: (a) weighting contributions of the grid points during the charge fitting by multiplying the $(\phi_i^{QC} - \phi_i^{FF})^2$ terms of the objective function by the electrostatic potential or a square of it, or (b) reducing the VDW radii of the atoms. Weighting of the grid points by the absolute value of the electrostatic potential, and especially the square of the electrostatic potential, resulted in a much better description of the electrostatic potential in the proximity of the EO atom, as seen in Figure 3, at the expense of overestimating the DME dipole moments, as seen in Table 5. On the other hand, reducing the VDW radii by 0.2−0.3 Å results in little change in the description of the electrostatic potential but changed the absolute values of the charges by as much as 0.03 e for oxygen and 0.04 e for hydrogen. The partial charges from the fits are presented in Table 6. The set of partial charges obtained using the least-squares minimization of the $\sum(\phi_i^{QC})^2(\phi_i^{QC} - \phi_i^{FF})^2$ objective function, i.e., the $(\phi_i^{QC})^2$ weighting function, provide the most satisfactory description of the electrostatic potential for the purpose of modeling PEO/Li^+ salts. To improve the description of the electrostatic potential close to the molecule, as well as far from it, one must include a set of the permanent

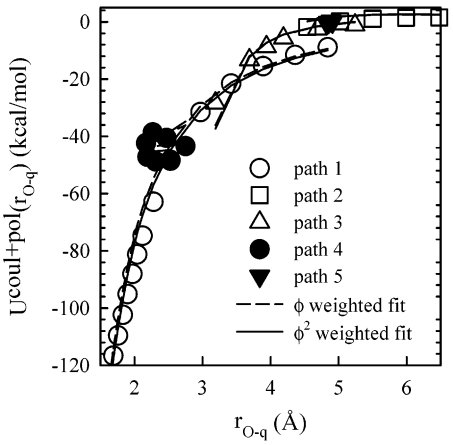

Figure 4. Total electrostatic energy (coulombic plus polarizable energy) as a function of the EO charge separation (r_{O-q}) for the tgt conformer of DME interacting with a positive unit test charge along the paths shown in Figure 1. Charges from the fits to the electrostatic potential with ϕ- and ϕ^2-weighting have been used.

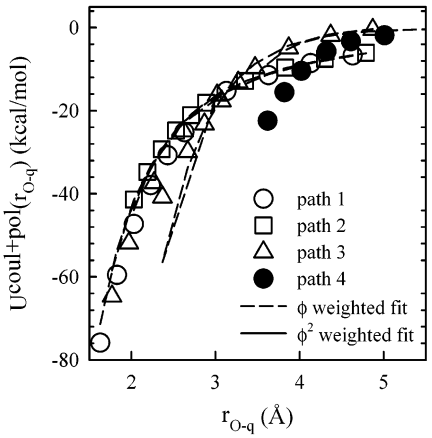

Figure 5. Total electrostatic energy (coulombic plus polarizable energy) as a function of EO charge separation (r_{O-q}) for a dimethyl ether interacting with a positive unit test charge along the paths shown in Figure 1. Charges from the fits to the electrostatic potential with ϕ- and ϕ^2-weighting have been used.

dipoles, quadrupoles, etc. and possibly lone pairs in the model, in addition to partial charges.[49,52] In this contribution, we limit ourselves to the simple point-charge model plus induced dipole many-body polarization, because it yields an adequate, albeit not excellent, description of the electrostatic potential and keeps computational cost of simulations down.

Figures 4 and 5 show that the force field can adequately reproduce the total quantum chemistry electrostatic energy (coulombic plus polarization) for DME and dimethyl ether if weighting of the electrostatic grid points is used during charge fitting.

C. Repulsion and Dispersion Parameters. The repulsion and dispersion parameters are typically obtained from experiments by fitting densities and heats of vaporization of oligomers,[50] fitting crystal structures,[51,52] or using vapor−liquid equilibrium data.[53] Obtaining the repulsion and dispersion parameters by fitting the complex energies of two representative model compounds using the HF level and correlated quantum chemistry methods is less popular. Here, we would like to examine the ability of quantum chemistry calculations to predict the repulsion and dispersion parameters accurately. This can be done by calculating the repulsion and dispersion contribution to the binding energy separately, using quantum chemistry, and comparing the results to the empirically determined repulsion and dispersion parameters.[51]

Previous work on noble gases[54] indicated that the basis set superposition error (BSSE)-corrected HF complex energies converge rather quickly as the basis set size increases, making calculation of repulsion contribution relatively easy. The dispersion (energy using the correlated method minus HF method) contribution to the complex energy is much more difficult to obtain; it requires the MP4 or coupled-cluster calculations with the triple-ζ and larger basis sets. We start with an easier task of determining the repulsion parameters from quantum chemistry calculations and then discuss the ways to obtain the dispersion parameters. The complex energy of a dimethyl ether dimer at the HF level can be approximated as a sum of the coulombic, many-body polarization and repulsion interactions. The first two contributions are adequately described by the previously determined charges and polarizabilities, leaving only the repulsion parameters as being unknown.

The binding energy with the exception of dispersion was calculated the following way. The geometry of the dimethyl ether dimer was optimized at the MP2/aug-cc-pvDz level. One of the dimethyl ether molecules then was shifted along path 1, as shown in Figure 6. The second path was generated by rotating a dimethyl ether by 180° and shifting it along path 2, as shown in Figure 6. The complexation energy was defined as the energy of the complex minus the energy of the individual molecules frozen at the complex geometry. The BSSE correction was performed using the counterpoise method.[55] The BSSE-corrected dimethyl ether dimer complex energy at the HF/aug-cc-pvDz level was the same as the HF/aug-cc-pvTz energy, within 0.01 kcal/mol, for the minimum configuration (path 1), indicating that the HF energy is essentially converged at the aug-cc-pvDz basis set.

The complex energies at the HF/aug-cc-pvDz level for the two paths are shown in Figure 6, along with the complex energies from the force field using the empirical repulsion parameters obtained by fitting poly(oxymethylene) (POM) crystal structures,[51] together with the quantum chemistry-based charges and polarizabilities. The force field with the empirical repulsion parameters and charges from the ϕ^2-weighted electrostatic potential fit can describe the most-important part of the dimethyl ether−dimethyl ether complexation (path 1, $r(O-O) \geq 3.9$ Å) calculated at the HF/aug-cc-pvDz level within 0.03 kcal/mol! The closer separations, with $r(O-O) = 3.5$ Å (path 1), are described within 0.09 kcal/mol, whereas the average absolute deviation of the force field complex energies from the HF/aug-cc-pvDz energies along the path 2 is 0.09 kcal/mol. The charges from the ϕ-weighted electrostatic potential fit yielded a slightly worse but comparable agreement, as shown in Figure 6. The excellent agreement between the force field and the HF/aug-cc-pvDz energies along the two paths indicates that the empirical repulsion parameters would be very similar to optimized quantum chemistry-based repulsion parameters and, therefore, could be used in our quantum chemistry-based PEO force field without any further modifications.

Accurate determination of the dispersion parameters from ab initio quantum chemistry calculations requires the use of large basis sets, generally beyond triple-ζ, and the inclusion of higher-order correlations beyond MP2, making it a daunting task. Nevertheless, it is interesting to compare the correlation (dispersion) energy of the empirical force field to that from the ab initio quantum chemistry calculations. The empirical dispersion parameters are taken from the POM force field[51] and are scaled by 7% to yield the correct density of diglyme liquid at

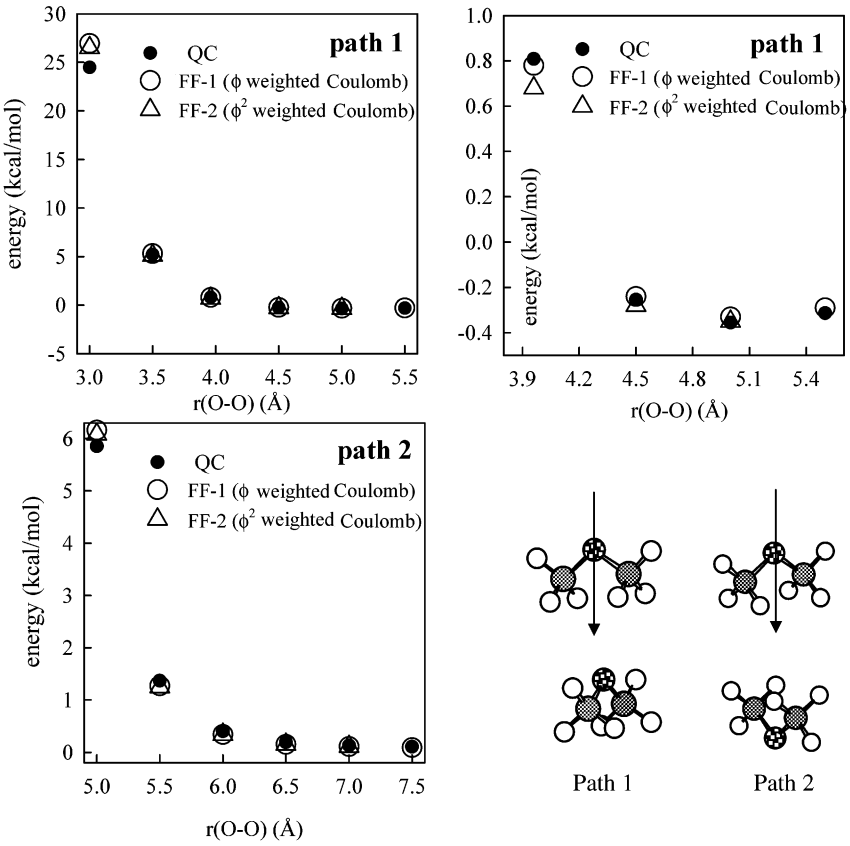

Figure 6. Complex energy of the dimethyl ether dimer at HF/aug-cc-pvDz level, as a function of the distance between EO atoms (r(O−O)) along the two paths and from molecular mechanics using the developed force fields.

TABLE 7: Repulsion (*A*) and Dispersion (*B* and *C*) Parameters for the Many-Body Polarizable and Two-Body PEO Force Fields

atom pair	A (kcal/mol)	B (Å^{-1})	C^a (kcal Å^{-6} mol^{-1})
C−C	14976.0	3.090	595.94 (637.6)
C−O	33702.4	3.577	470.18 (503.0)
C−H	4320.0	3.415	128.56 (137.6)
O−O	75844.8	4.063	370.96 (396.9)
O−H	14176.0	3.9015	97.16 (104.0)
H−H	2649.6	3.740	25.44 (27.22)

[a] Dispersion parameters for the two-body PEO force field are given in parentheses.

293 K, which is obtained from MD simulations using the MB polarizable force field. These modified empirical dispersion parameters are given in Table 7. The correlation energy from the quantum chemistry calculations for the dimethyl ether dimer was obtained by performing a double extrapolation (to the complete basis set limit and to the improved treatment of electron correlations) from the BSSE-corrected MP2/aug-cc-pvDz energies. First, the BSSE-corrected correlation energy at the MP2 level (i.e., MP2−HF) was extrapolated to the complete basis set limit using the previously found X^{-3} scaling,[13] based on the MP2/aug-cc-pvXz calculations with X = D, T, yielding the complete basis set limit correlation energy (MP2−HF) of −2.30 kcal/mol for the MP2/aug-cc-pvDz geometry. The MP2−HF correlation energy, using the complete basis set extrapolation, was 14.2% larger than that for the aug-cc-pvDz value. The second extrapolation takes into account the deficiency of the MP2 level in the treatment of electron correlations and involves scaling by the factor of (MP4/aug-cc-pvDz)/(MP2/aug-cc-pvDz) = 1.07. Thus, the double extrapolation for the correlation energy using these two scaling factors (MP4/aug-cc-pvDz)/(MP2/aug-cc-pvDz) and (MP2/complete basis set limit)/(MP2/aug-cc-pvDz) indicates that the correlation energy at the MP2/aug-cc-pvDz level should be multiplied by a factor of 1.22.

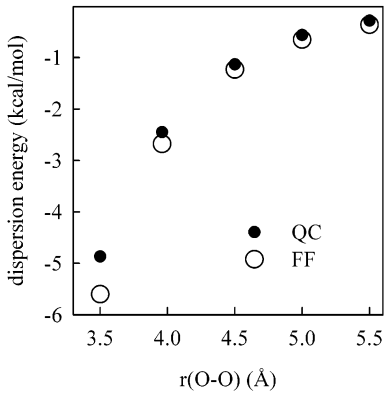

Figure 7. Dispersion (correlation) energy of the dimethyl ether dimer as a function of the distance between EO atoms r(O−O) from the quantum chemistry calculations and from the force field.

The correlation energy of a dimethyl ether dimer along path 1 for r(O−O) ≥ 3.5 Å obtained by double extrapolation is shown in Figure 7, together with the dispersion energy from the force field. The quantum chemistry predictions are 8%−23% (13%, on average) lower than the dispersion contribution from the empirical force field. These results agree well with the conclusions of benchmark calculations on He_2, Ne_2, and Ar_2 that reported that the BSSE-corrected complete basis set extrapolation of the MP4 complex energy was ∼10% below the empirical values,[54] which indicated that the dispersion parameters could be obtained with an accuracy on the order of 10% from ab initio quantum chemistry calculation, using the previously described double extrapolation scheme. Moreover,

TABLE 8: Valence Force Field Parameters for PEO

Bond Type		r_0 (Å)
C−O	constrained	1.4115
C−C	constrained	1.5075
C−H	constrained	1.1041
Bend Type	k^{BEND} (kcal mol^{-1} rad^{-2})	θ_0 (degrees)
C−C−H	85.8	110.10
H−C−H	77.0	109.47
O−C−H	112.0	109.48
C−O−C	149.0	108.05
O−C−C	172.0	108.54

scaling of the dispersion parameters obtained this way by a factor of 1.1 would yield dispersion parameters that are accurate to within a couple percent.

D. Parametrization of Dihedral, Bending, and Bonding Interactions. Although bond and bend force constants can be obtained by fitting vibrational frequencies of model PEO compounds, in this work, we simply took them from the previously developed nonpolarizable PEO force field,[24] whereas the equilibrium bond lengths and bending angles were fit to yield the best description of equilibrium geometries from molecular mechanics with those from the B3LYP/aug-cc-pvDz geometry optimizations for the tgt, ttt, and tgg conformers. The valence force field parameters are summarized in Table 8.

The dihedral parameters for the H−C−O−C angle were obtained by fitting quantum chemistry energies for the CH_3-group rotation of dimethyl ether at the MP2/aug-cc-pvDz//B3LYP/aug-cc-pvDz level (not shown). The O−C−C−H and H−C−C−H torsional parameters were taken from the previous nonpolarizable PEO force field.[24] We originally fitted the O−C−C−O and C−O−C−C torsional parameters to reproduce the conformational energetics of the most-important DME conformers and barriers between them, using two sets of the previously obtained charges, together with the polarizabilities and other nonbonded parameters, denoted as force fields FF-1 and FF-2 (see Table 9). The resulting force fields were able to describe the relative conformational energies of DME shown in Table 1 accurately, with an average deviation of 0.15 and 0.13 kcal/mol from the MP2/aug-cc-pvTz//MP2/aug-cc-pvDz QC energies (in boldface type in Table 1), respectively. Geometries of the most-important DME conformers from the force fields shown in Table 2 agree with those from the MP2/aug-cc-pvDz optimization (in boldface type in Table 2), with an average error of 3.5° and 3.7° for FF-1 and FF-2, respectively. These average deviations of the torsional angles from those at MP2/aug-cc-pvDz geometries are similar to the average deviation of the HF/aug-cc-pvDz geometries (4.4°) and that of the B3LYP/aug-cc-pvDz geometries (3.6°) from the MP2/aug-cc-pvDz geometries, which suggests that the force fields do a good job in reproducing the geometries of the most-important DME conformers. The description of the t−ϕ−t and t−g−ϕ rotational isomerization paths is shown in Figure 8. The lowest energy barriers (tgt/ttt, tg$^+$g$^-$/tgt, and ttt/ttg (not shown)) were described within 0.2 kcal/mol from the MP2/aug-cc-pvDz//B3LYP/aug-cc-pvDz energies, whereas the energies of the higher barriers (tgt/tgg and ttg/tg$^+$g$^-$) were underestimated by the force fields by 0.3−0.5 kcal/mol. We consider the FF-1 and FF-2 force field fits to quantum chemistry data to be good.

MD simulations of PEO with the FF-2 force field reported in the next paper of this series[56] indicate that PEO dynamics using this force field are somewhat slow. Therefore, we attempted to rectify this deficiency of the force field by refitting the torsional parameters to the barriers for conformational

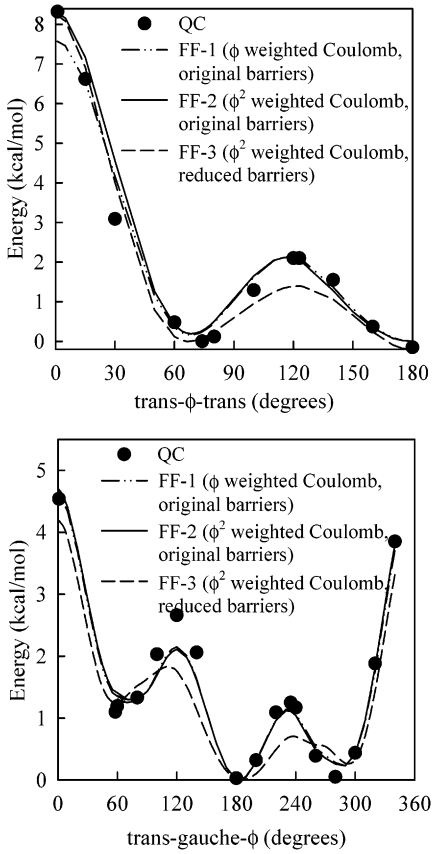

Figure 8. Relative conformational energy along the low-energy rotational isomerization paths for DME. Quantum chemistry points correspond to the MP2/aug-cc-pvDz//B3LYP/aug-cc-pvDz level energies.

transitions that were decreased by 0.3−0.9 kcal/mol, while keeping the partial charges and other force field parameters the same as those in the FF-2 force field. This force field will be called the FF-3 force field. The torsional parameters for this force field are given in Table 9. This barrier reduction is higher than the expected accuracy of the quantum chemistry calculations and, therefore, is considered to be an empirical adjustment. The FF-3 force field described the relative conformational energies and geometries with an accuracy that was similar to that for the FF-1 and FF-2 force fields (see Tables 1 and 2). The conformational isomerization paths for the FF-3 force field are shown in Figure 8, demonstrating the effect of lowering the barriers for conformational transitions in the FF-3 force field, compared to the FF-1 and FF-2 force fields. (See Table 9.)

The ability of the developed force fields to predict the relative conformational energies of a diglyme (a three-repeat-unit oligomer of ethylene oxide, CH_3-terminated, $C_6O_3H_{14}$) is shown in Table 10. The average deviation of the force fields conformational energies from the quantum chemistry values is 0.11−0.19 kcal/mol, with the maximum deviation of 0.41 kcal/mol. This accuracy is comparable to the accuracy of the quantum chemistry calculations for the diglyme molecule, which is expected to be ∼0.3−0.4 kcal/mol.

V. Two-Body Force Field Approximation

Analysis of the many-body polarizable contribution to the relative conformational energies of DME, using molecular mechanics, showed that the polarizability energy is small and contributes less than ±0.15 kcal/mol to the conformational energetics, relative to the ttt conformer. The induced dipole moment of the most-important DME conformers contributes

TABLE 9: Torsional Parameters for the PEO Force Fields (in the Order FF-1, FF-2, and FF-3)

	Torsional Parameter[a] (kcal/mol)				
type	$k^t(1)$	$k^t(2)$	$k^t(3)$	$k^t(4)$	$k^t(5)$
O−C−C−H	0.0	0.0	0.28[b]	0.0	0.0
H−C−C−H	0.0	0.0	0.28[b]	0.0	0.0
C−O−C−H	0.0	0.0	−0.73	0.0	0.0
O−C−C−O	0.25, 0.41, 0.47	−1.87, −2.10, −2.43	−0.43, −0.60, −0.36	−0.69, −0.82, −0.95	0.0, 0.0, −0.45
C−O−C−C	1.76, 1.76, 1.87	0.67, 0.67, 1.17	0.04, 0.04, 0.46	0.0, 0.0, −0.37	0.0, 0.0, 0.0

[a] If only one value is given, it is the same for all force fields. [b] Taken from ref 51.

TABLE 10: Relative Conformational Energies of Diglyme from ab Initio Quantum Chemistry and the Force Fields

	Relative Conformation Energy (kcal/mol)					
conformer	MP2/D95+(2df,p)//MP2/D95*	FF-1 MB	FF-1 TB	FF-2 MB	FF-3 MB	FF-3 TB
ttttt	0.0	0.0	0.0	0.0	0.0	0.0
tg^+ttt	0.03	−0.02	−0.02	−0.02	0.0	−0.01
tg^+g^-tt	0.01	0.27	0.28	0.21	0.15	0.13
tg^+g^+tt	0.83	1.04	0.98	1.07	0.87	0.80
ttg^+tt	1.15	1.14	1.03	1.11	1.31	1.13
tg^-tg^-tt	0.95	1.37	1.28	1.25	1.36	1.28
$tg^-g^+g^+tt$	1.10	1.35	1.18	1.36	1.46	1.22

10%−20% to the total dipole moment, which also indicates a relatively small effect of atomic polarizabilities on the electrostatic interactions and suggests that it is possible to turn off atomic polarizability and slightly increase the dispersion parameters to compensate for the induced dipole−permanent partial charge attraction that is not considered by the two-body force fields. Therefore, it reasonable to suggest that a nonpolarizable (or two-body force field, called TB) can be created from the corresponding many-body polarizable force field (called MB) by zeroing the polarizabilities and increasing the dispersion parameters by 7% to compensate in a mean-field sense for a decreased attraction and to keep the density of PEO oligomers the same for many-body polarizable and nonpolarizable force fields.[56]

We investigated the effect of increasing the dispersion and turning off the polarizability on equilibrium dihedral angles and conformational energetics for the FF-1 force field, as presented in Tables 2 and 1, respectively. The equilibrium dihedrals angles are different by $<1°$ between the MB and TB force fields. Conformational energetics of DME and diglyme are also very similar between the TB and MB force fields, with a maximum deviation of 0.15 kcal/mol for DME and 0.17 kcal/mol for diglyme for the FF-1 force field and 0.24 kcal/mol for diglyme for the FF-3 force field, whereas the average deviations of the conformational energies of the MB force field from the TB force field were 0.05−0.1 kcal/mol for DME and diglyme. Therefore, we conclude that, so far, there is little difference observed between the MB and TB force fields. In the next paper,[56] we will investigate, in detail, the effect of many-body polarizable interactions on the static, dynamic, and thermodynamic properties of PEO and its oligomers in a liquid (melt) phase.

VI. Conclusions

In this paper, we have presented a consistent methodology for developing quantum chemistry-based polymer force fields with many-body polarization interactions. Adequate levels of theory and basis sets for determining the relative conformational energetics, repulsion and dispersion nonbonded parameters, dipole moments, and molecular polarizability have been established. Repulsion parameters were accurately determined from Hartree−Fock (HF) calculations with relatively small basis sets, such as aug-cc-pvDz, whereas extrapolation to the complete basis set limit and the Møller−Plesset fourth-order (MP4) level of theory is required to obtain dispersion parameters within 10% of the empirical values obtained by fitting crystal structures of poly(oxymethylene), which is a compound whose structure is similar to that of poly(ethylene oxide) (PEO).

The B3LYP density functional, in conjunction with the aug-cc-pvDz basis set, yielded adequate polarizabilities and dipole moments of model ethers, whereas this functional with the aug-cc-pvDz basis set yielded dimethoxyethane (DME) relative conformational energies that were up to 1.3 kcal/mol different from MP2/aug-cc-pvDz energetics. Large deviations of the B3LYP functional from those of the MP2 calculations precluded its usage for accurate prediction of the conformational energetics, despite the B3LYP level conformational energetics being consistently closer to the MP2-level energetics than the HF energetics. The B3LYP geometries, on average, agreed better with the MP2 geometries than the HF geometries, suggesting that the B3LYP functional is preferred for geometry optimization, compared to the HF level, because computational time for the B3LYP and HF optimization is essentially the same.

Partial charges fitted to the electrostatic potential on a grid around PEO oligomers, with all points having equal weight in the fit, were found to underestimate the electrostatic potential in the proximity of atoms. Giving greater weight to the electrostatic grid points in the proximity of atoms by weighting the deviations of the force field electrostatic potential from the quantum chemistry values by the absolute value of the electrostatic potential (ϕ-weighting) or its square (ϕ^2-weighting) significantly improves the description of the electrostatic potential in the proximity of atoms by the force field, at the expense of overestimating the molecular dipole moment and the electrostatic potential relatively far from atoms. Inclusion of the permanent dipoles, quadrupoles, etc. and possibly lone pairs in the model must be considered in the future if a more accurate description of the electrostatic potential around the molecule is desired.

Finally, analysis of the many-body polarization contribution on the relative conformational energies showed that this energy term is small and contributes less than ± 0.15 kcal/mol to the relative conformational energies.

Acknowledgment. The authors are indebted to NASA (Grant No. NAG3 2624) and a subcontract from Lawrence Berkeley National Laboratory (LBL) (Subcontract No. 6515401) for financial assistance.

References and Notes

(1) Amiji, M.; Park, K. *Biomaterials* **1992**, *13*, 682.

(2) Jeon, S. I.; Lee, J. H.; Andrade, J. D.; de Gennes, P. G. *J. Colloid Interface Sci.* **1991**, *142*, 129.

(3) Harris, J. M. *Poly(Ethylene Glycol) Chemistry. Biotechnical and Biomedical Applications*; Plenum Press: New York and London, 1992.

(4) Harris, J. M.; Zalipsky, S. *Poly(Ethylene Glycol): Chemistry and Biological Applications*; ACS Symposium Series 680; American Chemical Society: Washington, DC, 1998.

(5) Morra, M.; Occhiello, E.; Garbassi, F. *Clin. Mater.* **1993**, *14*, 255.

(6) Espadas-Torre, C.; Meyerhoff, M. E. *Anal. Chem.* **1995**, *67*, 3108.

(7) Cappello, B.; Del Nobile, M. A.; La Rotonda, M. I.; Mensitieri, G.; Miro, A.; Nicolais, L. *Il Parmaco* **1994**, *49*, 809.

(8) Gray, F. M. *Polymer Electrolytes*; The Royal Society of Chemistry: Cambridge, U.K., 1997.

(9) Warriner, H. E.; Davidson, P.; Slack, N. L.; Schellhorn, M.; Eiselt, P.; Idziak, S. H. J.; Schmidt, H. W.; Safinya, C. R. *J. Chem. Phys.* **1997**, *107*, 3707.

(10) Rex, S.; Zuckermann, M. J.; Lafleur, M.; Silvius, J. R. *Biophys. J.* **1998**, *75*, 2900.

(11) Evans, E.; Rawicz, W. *Phys. Rev. Lett.* **1997**, *79*, 2379−2382.

(12) Rogers, R. D., Eiteman, M. A., Eds. *Aqueous Biphasic Separations*; Plenum Press: New York, 1995; pp 1−17.

(13) Smith, G. D.; Borodin, O.; Bedrov, D. *J. Comput. Chem.* **2002**, *23*, 1480.

(14) Bedrov, D.; Pekny, M.; Smith, G. D. *J. Phys. Chem. B* **1998**, *102*, 996.

(15) Trouw, F.; Bedrov, D.; Borodin, O.; Smith, G. D. *Chem. Phys.* **2000**, *261*, 137.

(16) Bedrov, D.; Borodin, O.; Smith, G. D. *J. Phys. Chem. B* **1998**, *102*, 5683.

(17) Bedrov, D.; Borodin, O.; Smith, G. D. *J. Phys. Chem. B* **1998**, *102*, 9565.

(18) Borodin, O.; Bedrov, D.; Smith, G. D. *Macromolecules* **2001**, *34*, 5687.

(19) Bedrov, D.; Smith, G. D. *J. Phys. Chem. B* **1999**, *103*, 3791.

(20) Bedrov, D.; Borodin, O.; Smith, G. D.; Trouw, F.; Mayne, C. *J. Phys. Chem. B* **2000**, *104*, 5151.

(21) Smith, G. D.; Bedrov, D.; Borodin, O. *J. Am. Chem. Soc.* **2000**, *122*, 9548.

(22) Smith, G. D.; Bedrov, D.; Borodin, O. *Phys. Rev. Lett.* **2000**, *85*, 5583.

(23) Halley, J. W.; Duan, Y.; Nielsen, B.; Redfern, P. C.; Curtiss, L. A. *J. Chem. Phys.* **2001**, *115*, 3957.

(24) Smith, G. D.; Jaffe, R. L.; Yoon, D. Y. *J. Phys. Chem.* **1993**, *97*, 12752.

(25) Neyertz, S.; Brown, D.; Thomas, J. O. *J. Chem. Phys.* **1994**, *101*, 10064.

(26) Lin, B.; Halley, J. W.; Boinske, P. T. *J. Chem. Phys.* **1996**, *105*, 1668.

(27) Müller-Plathe, F.; van Gunsteren, W. F. *J. Chem. Phys.* **1995**, *103*, 4745.

(28) Müller-Plathe, F. *Acta Polym.* **1994**, *45*, 259.

(29) Hyun, J.-K.; Dong, H.; Rhodes, C. P.; Frech, R.; Wheeler, R. A. *J. Phys. Chem. B* **2001**, *10*, 3329.

(30) Matsuura, H.; Miyazawa, T.; Machida, K. *Spectrochim. Acta, Part A* **1973**, *29A*, 771.

(31) Yoshida, H.; Kaneko, I.; Matsuura, H.; Ogawa, Y.; Tasumi, M. *Chem. Phys. Lett.* **1992**, *196*, 601.

(32) Yoshida, H.; Tanaka, T.; Matsuura, H. *Chem. Lett.* **1996**, 637.

(33) Inomata, K.; Abe, A. *J. Phys. Chem.* **1992**, *96*, 7934.

(34) Astrup, E. E. *Acta Chem. Scand., Series A* **1979**, *A33*, 655.

(35) Yoshida, H.; Matsuura, H. *J. Phys. Chem. A* **1998**, *102*, 2691.

(36) Tsuzuki, S.; Uchimaru, T.; Tanabe, K.; Hirano, T. *J. Phys. Chem.* **1993**, *97*, 1346.

(37) Jaffe, R. L.; Smith, G. D.; Yoon, D. Y. *J. Phys. Chem.* **1993**, *97*, 12745.

(38) Abe, A.; Furuya, H.; Mitra, M. K.; Hiejima, T. *Comput. Theor. Polym. Sci.* **1998**, *8*, 253.

(39) Kendall, R. A.; Dunning, T. H., Jr.; Harrison, R. J. *J. Chem. Phys.* **1996**, *96*, 6796.

(40) Frisch, M. J.; Trucks, G. W.; Schlegel, H. B.; Scuseria, G. E.; Robb, M. A.; Cheeseman, J. R.; Zakrzewski, V. G.; Montgomery, J. A., Jr.; Stratmann, R. E.; Burant, J. C.; Dapprich, S.; Millam, J. M.; Daniels, A. D.; Kudin, K. N.; Strain, M. C.; Farkas, O.; Tomasi, J.; Barone, V.; Cossi, M.; Cammi, R.; Mennucci, B.; Pomelli, C.; Adamo, C.; Clifford, S.; Ochterski, J.; Petersson, G. A.; Ayala, P. Y.; Cui, Q.; Morokuma, K.; Malick, D. K.; Rabuck, A. D.; Raghavachari, K.; Foresman, J. B.; Cioslowski, J.; Ortiz, J. V.; Stefanov, B. B.; Liu, G.; Liashenko, A.; Piskorz, P.; Komaromi, I.; Gomperts, R.; Martin, R. L.; Fox, D. J.; Keith, T.; Al-Laham, M. A.; Peng, C. Y.; Nanayakkara, A.; Gonzalez, C.; Challacombe, M.; Gill, P. M. W.; Johnson, B. G.; Chen, W.; Wong, M. W.; Andres, J. L.; Head-Gordon, M.; Replogle, E. S.; Pople, J. A. *Gaussian 98*, revision A.7; Gaussian, Inc.: Pittsburgh, PA, 1998.

(41) Becke, A. D. *J. Chem. Phys.* **1993**, *98*, 5648. Lee, C.; Yang, W.; Parr, R. G. *Phys. Rev. B* **1988**, *37*, 785.

(42) Lide, D. R., Ed. *CRC Handbook of Chemistry and Physics*, 81st ed.; CRC Press: Boca Raton, FL, 2000.

(43) Ruocco, G.; Sampoli, M. *Mol. Phys.* **1994**, *82*, 875

(44) Ma, B.; Lii, J.-H.; Allinger, N. L. *J. Comput. Chem.* **2000**, *21*, 813.

(45) Stout, J. M.; Dykstra, C. E. *J. Am. Chem. Soc.* **1995**, *117*, 5127.

(46) Breneman, C. M.; Wiberg, K. B. *J. Comput. Chem.* **1990**, *11*, 361.

(47) Borodin, O.; Smith, G. D. *Macromolecules* **1998**, *31*, 8396.

(48) Borodin, O.; Smith, G. D.; Jaffe, R. L. *J. Comput. Chem.* **2001**, *22*, 641.

(49) Cieplak, P.; Coldwell, J.; Kollman, P. *J. Comput. Chem.* **2001**, *22*, 1048.

(50) Watkins, E. K.; Jorgensen, W. L. *J. Phys. Chem. A* **2001**, *105*, 4118.

(51) Sorensen, R. A.; Liau, W. B.; Kesner, L.; Boyd, R. H. *Macromolecules* **1993**, *26*, 5213.

(52) Stone, A. J. *The Theory of Intermolecular Forces*; Oxford University Press: New York, 1996.

(53) Cui, S. T.; Siepmann, J. I.; Cochran, H. D.; Cummings, P. T. *Fluid Phase Equilib.* **1998**, *146*, 51.

(54) Woon, D. E. *J. Chem. Phys.* **1994**, *100*, 2838.

(55) van Duijneveldt, F. B.; van Duijneveldt-van de Rijdt, J. G. C. M.; van Lenthe, J. H. *Chem. Rev.* **1994**, *94*, 1873.

(56) Borodin, O.; Douglas, R.; Smith, G. D.; Trouw, F.; Petrucci, S. *J. Phys. Chem. B*, **2003**, *107*, 6813.